Desalination and Water Treatment
www.deswater.com
15 (2010) 76–83
March
1944-3994 / 1944-3986 © 2010 Desalination Publications. All rights reserved.
doi: 10.5004/dwt.2010.1670

Carbon nanotube-based nanocomposite desalination membranes from layer-by-layer assembly

Junwoo Park[a], Wansuk Choi[a], Jinhan Cho[b], Byung Hee Chun[a], Sung Hyun Kim[a], Ki Bong Lee[a]*, Joona Bang[a]*

[a]*Department of Chemical & Biological Engineering, Korea University, Anam-dong Seongbuk-gu, Seoul, 136-701 Korea*
Tel. +82 (2) 3290-4851; Fax +82 (2) 926-6102; email: kibonglee@korea.ac.kr, joona@korea.ac.kr
[b]*School of Advanced Materials Engineering, Kookmin University, Chungneung-dong, Songbuk-gu, Seoul 136-702, Korea*

Received 12 November 2009; Accepted in revised form 24 December 2009

ABSTRACT

In this work, we fabricated the nanocomposite reverse osmosis (RO) membranes based on the layer-by-layer (LbL) assembly of functionalized multi-walled carbon nanotubes (MWCNTs) and polyelectrolytes (PEs). The CNTs were incorporated to enhance the mechanical strength and the chlorine resistance of multilayered RO membranes. To fabricate the MWCNT-based nanocomposite multilayers, poly(allylamine hydrochloride) (PAH) and poly(acrylic acid) (PAA) were used as positively and negatively charged PEs, respectively, and the surface of MWCNTs was modified with carboxylic group. During the LbL assembly process, 1 wt % of carboxylated MWCNTs relative to PAA were used and $(MWCNT\text{-}PAA/PAH)_n$ multilayers membranes with 10, 15, and 20 bilayers were prepared. The existence of MWCNTs in multilayers was confirmed by thermogravimetric analysis (TGA), and we observed the improvement in thermal stability of multilayers after incorporation of MWCNTs. The salt rejection and permeate flux of these membranes were measured by a homemade RO test cell. To examine the chemical resistance to chlorine, $(MWCNT\text{-}PAA/PAH)_n$ multilayers were immersed in 3,000 ppm sodium hypochloride (NaOCl) solutions for 4 h. Consequently, it was found that the salt rejection of $(MWCNT\text{-}PAA/PAH)_n$ membranes decreases by 16.2%, 15.2% and 9.9% for 10, 15 and 20 bilayers, respectively, while the conventional polyamide membrane exhibited 21.8% decreases in the salt rejection.

Keywords: Desalination; Multi-walled carbon nanotube; Polyelectrolytes; Nanocomposite multilayers

1. Introduction

Recently, a drought continues in many areas in the world due to the global problem such as the global warming or El Nino's effect or the uncontrolled deforestation, causing the water-shortage problems in many countries. To solve this problem, many efforts are now devoted to secure the water source from various strategies, i.e., constructing a dam, recycling used water, developing the underground water, desalination of seawater, etc. Among these efforts, the desalination process is one of the most promising methods for alternative sources of water in the next generation. Currently, desalination of seawater can be performed via two processes: distillation and separation by reverse osmosis (RO) membranes. Since the conventional distillation requires a lot of energy to

* Corresponding author.

Presented at SeaHERO Academic Workshop on Development and Optimization of SWRO Desalination Systems
Korea University, Seoul, Korea, November 13–14, 2009

distill the seawater, RO membranes have now attracted much attention as an alternative method for the desalination process [1–4].

RO membranes have been developed from 1960s, and cellulose acetate and polyamide were mainly used as materials for the selective layer in RO membranes [5]. Cellulose acetate is a hydrophilic material and hence it is advantageous for preventing the biofouling problems. However, this material does not have mechanical strength and chemical resistance, and hence RO membranes made from cellulose acetate cannot be used for a long-term operation. Alternatively, polyamide-based RO membranes are widely used these days, as they have better mechanical strength and durability. In this case, the selective layer of polyamide is prepared by interfacial polymerization between the amine monomers (e.g., 1,3-benzenediamine) and aromatic acyl chloride monomers (e.g., trimesoyl chloride) to form a thin layer of densely crosslinked amide network. Consequently, commercialized RO membranes from polyamide show salt rejection of >99% and they were employed for the most of desalination RO processes. However, it has been pointed out that polyamide-based RO membranes have limitations in low permeate flux, biofouling, and weak chemical resistance to chlorines, etc. To solve these problems, several strategies have been proposed such as coating the surface of RO membranes with chemicals having high chemical resistance or modifying polyamide with various functional groups.

Recently, nanocomposite membranes have been suggested as promising candidates for RO membranes in the next generation [5–9]. In this case, the mechanical strength and chemical resistance can be enhanced by an incorporation of a small amount of inorganic nanoparticles into the selective layers. Among several possible components in nanocomposites, carbon nanotubes (CNTs) have been considered as an excellent candidate due to their remarkable mechanical strength, optical, and electrical properties. Therefore, CNTs are extensively employed in many areas with various applications, i.e., energy storage media [10–13], additives for improvement of mechanical strength [14–16], chemical sensors [17–19], and in biological applications [20–22]. As a representative example of nanocomposite membranes, CNTs have been dispersed within the polymer matrix to fabricate the multilayered nanocomposite membranes demonstrating the improved properties for various applications while the flexibility of nanocomposites is retained [23–30].

Previously, we introduced a novel method to fabricate desalination RO membranes from layer-by-layer (LbL) assembled polyelectrolytes (PEs) multilayers, using poly(allylamine hydrochloride) (PAH) and poly(acrylic acid) (PAA) as positively and negatively charged PEs, respectively [31]. By controlling the pH-condition during the deposition step followed by thermal crosslinking, we found the optimal structures for desalination membranes, i.e., membranes should contain a large amount of freely charged groups with densely-packed structures via crosslinking. In this work, we extend the LbL assembled RO membrane to fabricate nanocomposite RO membranes using multi-walled carbon nanotubes (MWCNTs) as additives. By using MWCNTs as inorganic components, the desalination performance and chemical resistance of these membranes were examined.

2. Materials and methods

2.1. Materials

Poly(acrylic acid) (PAA) (Polysciences, Mw = 100,000 g/mol) was used as anionic polyelectrolytes (PE). On the other hand, poly(allylamine hydrochloride) (PAH) (Aldrich, Mn = 56,000 g/mol) (Aldrich, Mw = 200,000–350,000 g/mol) was used as a cationic PE. An asymmetric porous polysulfone membrane (Trisep, UE50, Mw = 100,000 g/mol) was used as a substrate to construct the LbL multilayers. Multi-walled carbon nanotubes (MWCNTs) were purchased from Iljin CNT, and the average diameter and length were 9–12 nm and 10–15 μm, respectively.

2.2. Preparation of carboxylated MWCNTs and polyelectrolyte solution

To use MWCNTs in the LbL assembly, the surface of MWCNTs was carboxylated as described elsewhere [32]. First, MWCNTs were dispersed in a mixture of 1 M H_2SO_4 and 1 M HNO_3 (3:1 by volume), and heated to 70°C for overnight with reflux. The MWCNTs were then separated by centrifugation for 10 min at 10,000 rpm, followed by sonicating with deionized water. This step was repeated for at least three times. The resulting carboxylated MWCNTs were dried for 12 h under vacuum.

To anionic PAA aqueous solution (1.0 mg/mL), 1 wt% of carboxylated MWCNTs were mixed and sonicated for 3 h. As cationic PAH solution, the concentration was also adjusted to 1.0 mg/mL. The pH of MWCNT/PAA and PAH solutions were controlled by 0.1 M HCl and NaOH.

2.3. MWCNT/polyelectrolyte(MWCNT/PE) membranes formation

For deposition of LbL assembled MWCNT/PE multilayers onto the polysulfone (PSf) substrates, negatively charged PSf substrates were prepared by a treatment with 0.5 M H_2SO_4 solution at 80°C for 30 min. Then, the LbL assembled MWCNT/PE multilayers were fabricated onto the PSf substrates, by alternating deposition of oppositely charged PAH and MWCNT/PAA solutions. As shown in Fig. 1, The substrates were first dipped in the cationic PAH solution for 10 min, washed twice in deionized water for 1 min each, and air-dried with a gentle stream of nitrogen. The anionic MWCNT/PAA were then deposited onto the cationic PE-coated substrates by adsorption for 10 min,

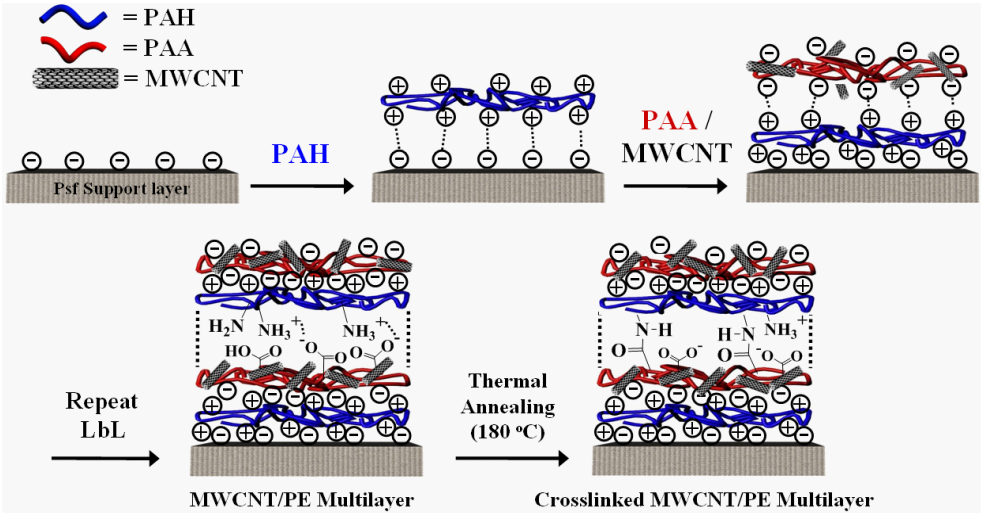

Fig. 1. Schematic illustration of the fabrication of nanocomposite $(MWCNT\text{-}PAA/PAH)_n$ multilayers via layer-by-layer assembly on polysulfone substrate.

washed in deionized water and air-dried. This process was repeated until the desired number of bilayers had been deposited. To impose the chemical crosslinking between PAH and MWCNTs/PAA layers, the $(MWCNT\text{-}PAA/PAH)_n$ multilayer membranes were heated to 180°C for 1 h under vacuum.

2.4. Characterization of membranes

The existence of carboxylic acid group in MWCNTs was analyzed by Fourier Transform Infrared (FT-IR) spectroscopy. FT-IR spectra were taken using a FTIR-200 spectrometer (JASCO Corporation) with CaF_2 window. The film thicknesses of the $(MWCNT\text{-}PAA/PAH)_n$ multilayers on silicon substrates were measured using by ellipsometry (Gaertner Scientific Corp., L2W15S830) using 632.8 nm He-Ne laser light. The surface morphology of the (MWCNT-PAA/PAH)n multilayers was examined by Field Emission-Scanning Electron Microscopy (FE-SEM, Hitachi, S-4300). Thermogravimetric analysis (TGA-Q50, TA Instrument LTD.) was used to investigate the existence of MWCNTs in $(MWCNT\text{-}PAA/PAH)_n$ multilayers and also their thermal stability. In this case, powders from the selective layers, $(MWCNT\text{-}PAA/PAH)_n$ multilayers, were obtained by scrubbing the membranes with doctor blade. TGA was fitted to a N_2 purge gas from ambient temperature to 1000°C at a heating rate of 10°C/min.

2.5. Operation condition

RO performance of $(MWCNT\text{-}PAA/PAH)_n$ multilayers was investigated using a homemade RO test system described previously [31]. The RO membranes were placed in a pressure chamber (effective area for the membrane cell = 13.85 cm^2; pressure = 15.5 bar). The ionic salt (NaCl) concentration and flux in the feed water were fixed to 2000 ppm and 333 $L/m^2 \cdot h$, respectively, at room temperature. At the bottom the cell was equipped with an outlet for the permeate solution. The ion concentration of the permeate was measured using the ionic conductivity meter (EUTECH, PC650). The salt rejection and permeate flux of RO membranes were calculated using the following equations:

$$\text{Salt rejection (\%)} = \left(1 - \frac{\text{permeate conductance}}{\text{feed conductance}}\right) \times 100 \quad (1)$$

$$\text{Permeate flux} = \frac{\text{permeate (L)}}{\text{membrane}\left(\text{m}^2\right) \times \text{time (h)}} \quad (2)$$

To test the chemical resistance to chlorine, the RO membranes after the first test were dipped into 3,000 ppm sodium hypochloride (NaOCl) solution for 4 h. The membranes were then washed with deionized water and tested again. Consequently, the salt rejection and permeate flux before and after treating with NaOCl were compared. Also, the chemical resistance of $(MWCNT\text{-}PAA/PAH)_n$ multilayers was compared with conventional polyamide-based membrane, which is prepared by interfacial polymerization between 1,3-benzenediamine and trimesoyl chloride according to the standard protocol established.

3. Results and discussion

In original MWCNT powders, the individual MWCNTs are highly entangled and physically agglomerated. To use them for various applications in a controlled manner, the surface of MWCNTs was chemically treated to disperse in various media. To use the MWCNTs in LbL assembly, we treated the MWCNTs with a mixture of

H_2SO_4 and HNO_3 to impose the negative charge on the surface with carboxylic acid group. It was observed that the resulting carboxylated MWCNTs are well dispersed in water and they are stable for several weeks without any agglomeration. Fig. 2 shows the FT-IR spectra of MWCNTs before and after modification with carboxylic acid groups. There are no particular peaks before modification, as only aromatic carbons are present in MWCNTs. After treatment with a mixture of H_2SO_4 and HNO_3, it is apparent that several peaks appear due to a carboxylation of MWCNTs. From Fig. 2, the FT-IR spectra confirms the presence of carbonyl group (–C=O in –COOH at 1703 cm^{-1}), carboxylate group (–COO- at 1568 cm^{-1}), and broad peak from –OH group in carboxylic acid group at 2500–3500 cm^{-1}.

For deposition of LbL assembled MWCNT/PE multilayers, 1 wt % of carboxylated MWCNTs were mixed with anionic PAA solutions. Fig. 3a shows the films thickness of MWCNT/PE multilayers with increasing the number of bilayers deposited on the silicon substrates. As previously established, MWCNT/PE multilayers were deposited under a condition of pH 7.5 for PAH and pH 3.5 for MWCNTs/PAA, to produce the thickest individual layers [31]. In this case, the film thickness increases from 2 nm for 1 bilayer to 280 nm for 10 bilayers, showing an exponential growth, which is typical of LbL deposition of PEs in multilayers. Under the same pH conditions, the MWCNT/PE multilayers were fabricated on PSf substrates that are typically used as supporting membranes for commercial RO membranes. After treating the surface of PSf substrates with H_2SO_4 solution to impose a negative charge, the MWCNT/PE multilayers, (MWCNT-PAA/PAH)n, with 10, 15, and 20 bilayers were prepared. The $(MWCNT\text{-}PAA/PAH)_n$ multilayer membranes were then heated to 180°C for 1 h under vacuum to induce the amide crosslinking between MWCNT-PAA/PAH layers,

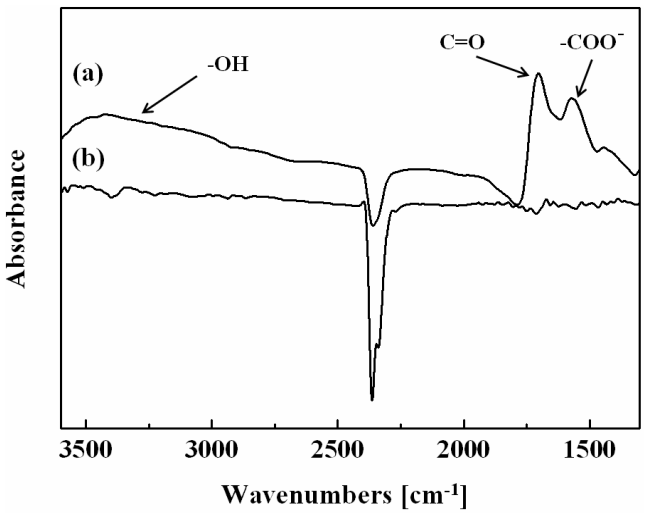

Fig. 2. FT-IR spectra of (a) carboxylated and (b) original MWCNTs.

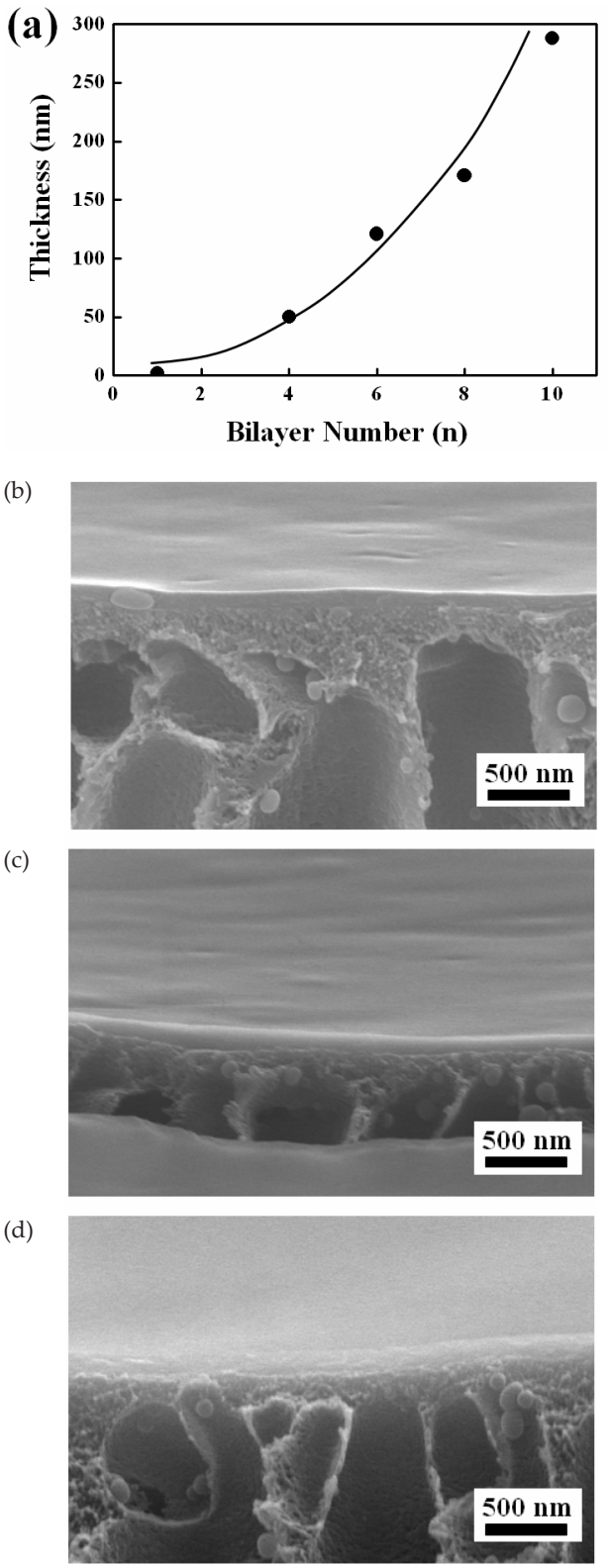

Fig. 3. (a) Film thickness of LbL assembled $(MWCNT\text{-}PAA/PAH)_n$ multilayers on silicon substrate, measured by ellipsometry. Cross-sectional SEM images of $(MWCNT\text{-}PAA/PAH)_n$ multilayers prepared on polysulfone substrates. (b), (c), and (d) correspond to the bilayer number of 10, 15, and 20, respectively.

as described previously [31]. Figs. 3b–3d correspond to the cross-sectional SEM images of crosslinked (MWCNT-PAA/PAH)$_n$ multilayer membranes with 10, 15, and 20 bilayers. The thickness of (MWCNT-PAA/PAH)$_n$ multilayers are 200 nm, 250 nm, and 310 nm, respectively. Note that the film thickness significantly decreases upon thermal treatment due to the formation of densely crosslinked structures.

The existence of MWCNTs and the thermal property of (MWCNT-PAA/PAH)$_n$ multilayers were investigated by TGA as shown in Fig. 4. For pure MWCNTs, they are thermally stable up to 750°C and then a small fraction (<20%) is decomposed. In contrast, (PAH/PAA)$_n$ membranes show a sharp decrease in a temperature range between 420°C and 510°C. This is due to a thermal decomposition of (PAH/PAA)$_n$ multilayers. Also, the membranes shows a continuous decreases up to 420°C with a small bump around 200°C, which can be attributed to the decomposition of residual solvents in multilayers or lower molecular portions of PSf in supporting layers. This behavior is similar in the case of (MWCNT-PAA/PAH)$_n$ multilayers. However, there is a remarkable change in the thermal decomposition in the region of 420–510°C. In (MWCNT-PAA/PAH)$_n$ multilayers, it can be clearly seen that the thermal decomposition is significantly retarded and it continues until the temperature reaches ~750°C. This result strongly supports that the MWCNTs were well embedded in multilayers and the thermal stability of (MWCNT-PAA/PAH)$_n$ multilayers is much more improved by an addition of small amount of MWCNTs. The enhanced thermal stability of the nanocomposite multilayers could be predicted based on many previous examples of nanocomposites containing CNTs [33–35]. We believe that the thermal stability of (MWCNT-PAA/PAH)$_n$ multilayers shown in Fig. 4 is due to the strong electrostatic interaction and covalent bonding between carboxylated MWCNTs and PEs (i.e., PAA and PAH) matrix.

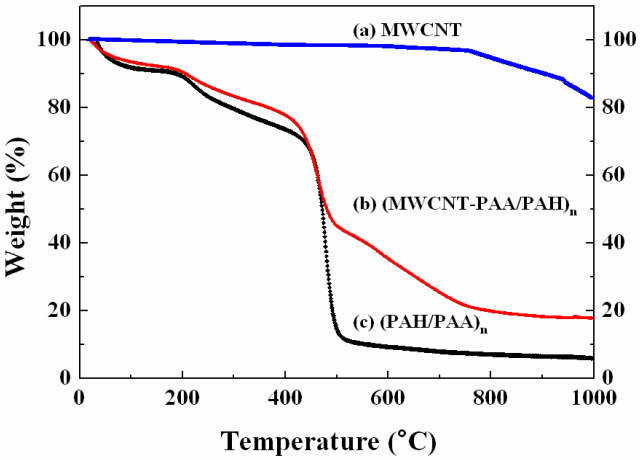

Fig. 4. TGA traces of (a) original MWCNTs, (b) (MWCNT-PAA/PAH)$_n$ multilayers, and (c) (PAA/PAH)$_n$ multilayers. The scan rate was 10°C/min.

The salt rejection and the permeate flux of (MWCNT-PAA/PAH)$_n$ multilayers were measured using a home-made RO test system. For all experiments, the ionic salt (NaCl) concentration and flux in the feed water were fixed to 2,000 ppm and 333 L/m^2·h, respectively. To find the optimal conditions for nanocomposite (MWCNT-PAA/PAH)$_n$ multilayers, the amount of MWCNTs and the number of bilayers were varied. Before measurements, (MWCNT-PAA/PAH)$_n$ multilayers were thermally crosslinked to induce the densely packed structures. When 5 wt % of MWCNTs were incorporated in (MWCNT-PAA/PAH)$_{10}$ multilayers, it was found that there exist some defects in the membrane, which is from the agglomeration of MWCNTs. In this case, the salt rejection and the permeate flux were 58% and 3.5 L/m^2·h, respectively (data not shown). The low salt rejection for (MWCNT-PAA/PAH)$_{10}$ multilayers can be attributed to the defects of aggregated MWCNTs, which allows NaCl salts to pass though the membranes. When 1 wt % of MWCNTs were incorporated in (MWCNT-PAA/PAH)$_{10}$ multilayers, the membranes exhibit almost defect-free structures without any agglomeration of MWCNTs. Fig. 5 shows the salt rejections and the permeate fluxes for (MWCNT-PAA/PAH)$_n$ multilayers containing 1 wt % of MWCNTs with the 10, 15, and 20 bilayers as a function of operating time. After operating for ~60 min, the salt rejection and the permeate flux were stabilized, and it was observed that all membranes exhibit the similar performance regardless of the number of bilayers. In this case, the salt rejections and the fluxes of (MWCNT-PAA/PAH)$_n$ multilayers containing 1 wt % of MWCNTs were 90.4% and 2.6 L/m^2·h for n = 10, 89.6% and 3.6 L/m^2·h for n = 15, and 91.2% and 2.1 L/m^2·h for n = 20, respectively. When the multilayers with 5 bilayers, (MWCNT-PAA/PAH)$_5$, were prepared, the salt rejection was only ~50–60%, implying that the films are too thin to function as the RO membranes. Therefore, it can be concluded that 10 bilayers would be the optimal structure with the minimum number of bilayers in (MWCNT-PAA/PAH)$_n$ multilayers, in terms of RO performance.

To test the chemical resistance to chlorine, the nanocomposite (MWCNT-PAA/PAH)$_n$ multilayers were immersed in 3,000 ppm sodium hypochloride (NaOCl) solution for 4 h, and then the salt rejections were compared. To quantitatively compare the chemical resistance of (MWCNT-PAA/PAH)$_n$ multilayers, we also prepared the polyamide RO membrane by interfacial polymerization between 1,3-benzenediamine and trimesoyl chloride. For the conventional polyamide RO membranes, it has been well known that they are weak to the chlorines. When the amide bonds are exposed to the chlorine, the N–H bond is readily chlorinated and oxidized to the quinoid structure by hydrolysis reaction with water. This reaction can occur in chainwise manner to degrade the amide network in the RO membranes. Therefore, the chlorination in polyamide

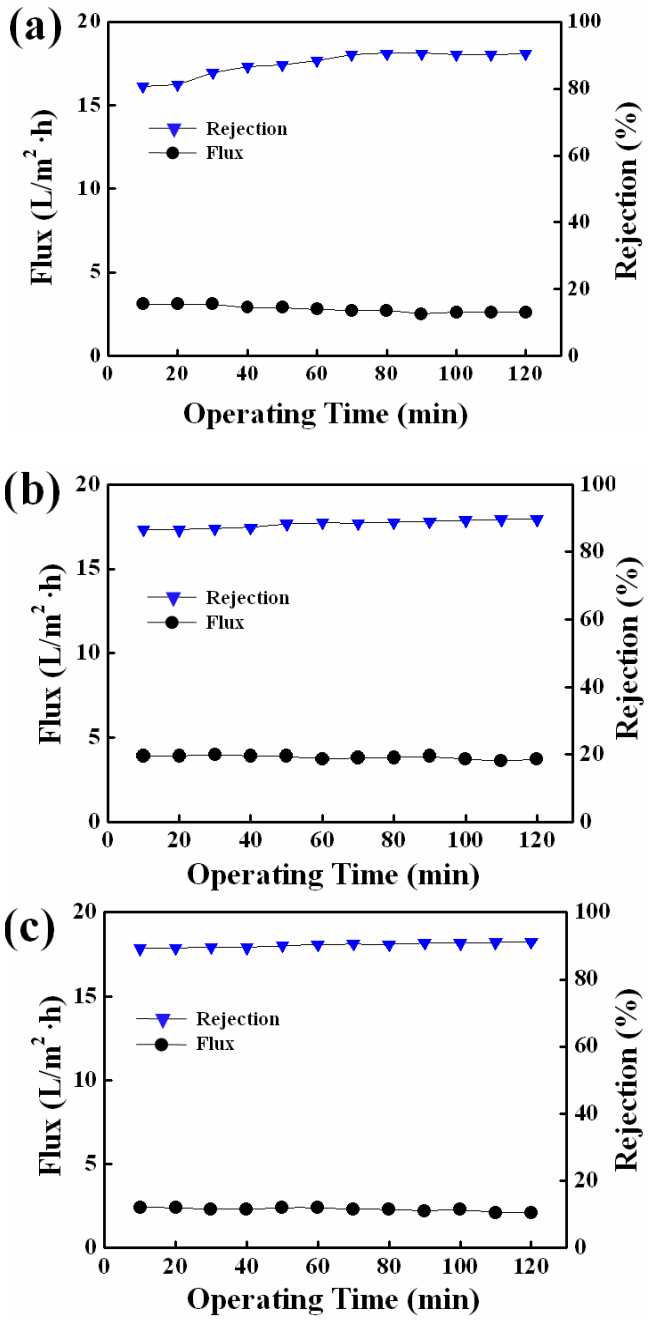

Fig. 5. Plot of salt rejection and permeate flux as a function of operation time for (a) $(MWCNT\text{-}PAA/PAH)_{10}$, (b) $(MWCNT\text{-}PAA/PAH)_{15}$, and (c) $(MWCNT\text{-}PAA/PAH)_{20}$ multilayers.

membranes results in serious defects and hence the salt rejection will significantly decrease. In our system, we expect that an incorporation of inorganic MWCNT can enhance the chemical resistance as well as the thermal stability, due to the electrostatic interaction and the covalent bonding between MWCNTs and polymer matrix. Fig. 6 shows the salt rejection of RO membranes before and after treating with NaOCl solution. For the polyamide membrane, it was observed that the salt rejection decreases by 21.8% (from 98.3% to 76.5%) upon chlorination. However, $(MWCNT\text{-}PAA/PAH)_n$ multilayers exhibit a decrease in the salt rejection by 16.2% (from 90.4% to 74.2%), 15.2% (from 89.6% to 74.4%), and 9.9% (from 91.2% to 82.4%), for $n = 10$, 15, and 20, respectively. The chlorine resistance should be closely related to the relative amount of decrease in the salt rejection after the chlorination, because the decrease in the salt rejection would mainly result from the defects in the membrane structures. In this regard, it can be concluded that $(MWCNT\text{-}PAA/PAH)_n$ multilayers show the better chlorine resistance than the polyamide membranes. Also, an increase in the number of bilayers leads to the less decrease in the salt rejection after chlorination, i.e., the better chlorine resistance. Therefore, the optimal structure in our system is $(MWCNT\text{-}PAA/PAH)_{20}$ multilayers, as they show the similar RO performance as 10 and 15 bilayers, but have the better chlorine resistance.

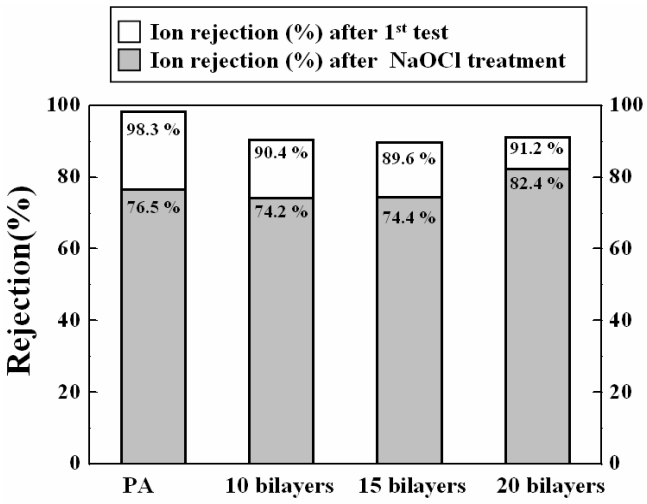

Fig. 6. Plot of salt rejection for polyamide membrane, $(MWCNT\text{-}PAA/PAH)_{10}$, $(MWCNT\text{-}PAA/PAH)_{15}$, $(MWCNT\text{-}PAA/PAH)_{20}$ multilayers before and after treatment with 3,000 ppm NaOCl solutions.

4. Conclusions

In this work, we fabricated the nanocomposite multilayered RO membranes from layer-by-layer assembly of carboxylated MWCNTs and polyelectolytes (PAA and PAH). The structure of $(MWCNT\text{-}PAA/PAH)_n$ multilayers was characterized by ellipsometry and FE-SEM. The existence of MWCNTs in multilayers was confirmed by TGA and it was found that an incorporation of 1 wt % MWCNTs significantly improves the thermal stability of nanocomposite $(MWCNT\text{-}PAA/PAH)_n$ multilayers, due to the strong electrostatic interaction and covalent bonding between carboxylated MWCNTs and PEs. The chlorine resistance of these nanocomposite membranes

was examined by treating with 3,000 ppm NaOCl solutions. In this case, they exhibited the improved resistance to chlorine comparing to the conventional polyamide RO membranes, as evidenced by the less decrease in the salt rejection after NaOCl treatments. For nanocomposite $(MWCNT\text{-}PAA/PAH)_n$ multilayers, the salt rejection decreases by 16.2%, 15.2%, and 9.9% for 10, 15, and 20 bilayers, respectively, whereas 21.8% of decrease in the salt rejection was observed in the conventional polyamide membranes. We anticipate that further improvement of these nanocomposite RO membranes can be achieved by employing different functional groups on the surface of MWCNTs, or optimizing the amount of MWCNTs incorporated, etc. Our approach for the well-defined nanocomposite RO membrane via LbL assembly can provide a firm basis for designing the highly efficient RO membranes with good chemical resistance that overcome the disadvantage of currently used RO membranes.

Acknowledgements

This research was supported by a grant (07seaheroB02-03) from the Plant Technology Advancement Program funded by the Ministry of Land, Transport and Maritime Affairs of the Korean government.

References

[1] C.Y. Tang, Y.-N. Kwon and J.O. Leckie, Effect of membrane chemistry and coating layer on physiochemical properties of thin film composite polyamide RO and NF membranes: I. FTIR and XPS characterization of polyamide and coating layer chemistry, Desalination, 242 (2009) 149–167.

[2] R.J. Petersen, Composite reverse osmosis and nanofiltration membranes, J. Membr. Sci., 83 (1993) 81–150.

[3] C.R. Bartels, M. Wilf, K. Andes and J. Iong, Design considerations for wastewater treatment by reverse osmosis, Water. Sci. Technol., 51 (2005) 473–482.

[4] K. Taori, V.J. Paul and H. Luesch, Structure and activity of largazole, a potent antiproliferative agent from the Floridian marine cyanobacterium *Symploca* sp., J. Am. Chem. Soc., 130 (2008) 1806–1807.

[5] B.-H. Jeong, E.M. Van Hoek, Y. Yan, A. Subramani, X. Huang, G. Hurwitz, A.K. Ghosh and A. Jawor, Interfacial polymerization of thin film nanocomposites: A new concept for reverse osmosis membranes, J. Membr. Sci., 294 (2007) 1–7.

[6] L. Lianchao, W. Baoguo, T. Huimin, C. Tianlu and X. Jiping, A novel nanofiltration membrane prepared with PAMAM and TMC by in situ interfacial polymerization on PEK-C ultrafiltration membrane, J. Membr. Sci., 269 (2006) 84–93.

[7] M. Zhou, P.R. Nemade, X. Lu, X. Zheng, E.S. Hatakeyama, R.D. Noble and D.L. Gin, New type of membrane material for water desalination based on a cross-linked bicontinuous cubic lyotropic liquid crystal assembly, J. Am. Chem. Soc., 129 (2007) 9574–9575.

[8] K. Sint, B. Wang and P. Král, Selective ion passage through functionalized graphene nanopores, J. Am. Chem. Soc., 130 (2008) 16448–16449.

[9] B. Corry, Designing carbon nanotube membranes for efficient water desalination, J. Phys. Chem. B, 112 (2008) 1427–1434.

[10] F. Leroux, K. Metenier, S. Gautier, E. Frackowiak, S. Bonnamy and F. Beguin, Electrochemical insertion of lithium in catalytic multi-walled carbon nanotubes, J. Power Sources, 81 (1999) 317–322.

[11] M. Sato, A. Noguchi, N. Demachi, N. Oki and M. Endo, A mechanism of lithium storage in disordered carbons, Science, 264 (1994) 556–558.

[12] E. Kymakis and G.A.J. Amaratunga, Carbon nanotubes as electron acceptors in polymeric photovoltaics, Rev. Adv. Mater. Sci., 10 (2005) 300–305.

[13] P.J. Britto, K.S.V. Santhanam, A. Rubio, A. Alonso and P. M. Ajayan, Improved charge transfer at carbon nanotube electrodes, Adv. Mater., 11 (1999) 154–157.

[14] M.M.J. Treacy, T.W. Ebbesen and J.M. Gibson, Exceptionally high Young's modulus observed for individual carbon nanotubes, Nature, 381 (1996) 678–681.

[15] A. Cao, D.L. Dickrell, W.G. Sawyer, M.N. Ghasemi-Nejhad and P.M. Ajayan, Super-compressible foamlike carbon nanotube films, Science, 310 (2005) 1307–1310.

[16] V.P. Veedu, A. Cao, X. Li, K. Ma, C. Soldano, S. Kar, P.M. Ajayan and M.N. Ghasemi-Nejhad, Multifunctional composites using reinforced laminae with carbon-nanotube forests, Nature Mater., 5 (2006) 457–462.

[17] J. Kong, N.R. Franklin, C. Zhou, M.G. Chapline, S. Peng, K. Cho and H. Dai, Nanotube molecular wires as chemical sensors, Science, 287 (2000) 622–625.

[18] P.W. Barone, S. Baik, D.A. Heller and M.S. Strano, Near-infrared optical sensors based on single-walled carbon nanotubes, Nature Mater., 4 (2005) 86–92.

[19] K. Bradley, J.C.P. Gabriel, A. Star and G. Grüner, Short-channel effects in contact-passivated nanotube chemical sensors, Appl. Phys. Lett., 83 (2003) 3821–3823.

[20] D.A. Heller, E.S. Jeng, T.K. Yeung, B.M. Martinez, A.E. Moll, J.B. Gastala and M.S. Strano, Optical detection of DNA conformational polymorphism on single-walled carbon nanotubes, Science, 311 (2006) 508–511.

[21] N.W.S. Kam, T.C. Jessop, P.A. Wender and H. Dai, Nanotube molecular transporters: Internalization of carbon nanotube-protein conjugates into mammalian cells, J. Am. Chem. Soc., 126 (2004) 6850–6851.

[22] R.J. Chen, Y. Zhang, D. Wang and H. Dai, Noncovalent sidewall functionalization of single-walled carbon nanotubes for protein immobilization, J. Am. Chem. Soc., 123 (2001) 3838–3839.

[23] A.A. Mamedov, N.A. Kotov, M. Prato, D.M. Guldi, J.P. Wicksted and A. Hirsch, Molecular design of strong single-wall carbon nanotube/polyelectrolyte multilayer composites, Nat. Mater., 1 (2002) 190–194.

[24] D. Chattopadhyay, I. Galeska and F. Papadimitrakopoulos, A route for bulk separation of semiconducting from metallic single-wall carbon nanotubes, J. Am. Chem. Soc., 123 (2001) 9451–9452.

[25] A.B. Artyukhin, O. Bakajin, P. Stroeve and A. Noy, Layer-by-layer electrostatic self-assembly of polyelectrolyte nanoshells on individual carbon nanotube templates, Langmuir, 20 (2004) 1442–1448.

[26] J.H. Rouse and P.T. Lillehei, Electrostatic assembly of polymer/single walled carbon nanotube multilayer films, Nano Lett., 3 (2003) 59–62.

[27] S.-C.J. Huang, A.B. Artyukhin, Y. Wang, J.W. Ju, P. Stroeve and A. Noy, Persistence length control of the polyelectrolyte layer-by-layer self-assembly on carbon nanotubes, J. Am. Chem. Soc., 127 (2005) 14176–14177.

[28] M. Michel, A. Taylor, R. Sekol, P. Podsiadlo, P. Ho, N. Kotov and L. Thompson, High-performance nanostructured membrane electrode, assemblies for fuel cells made by layer-by-layer assembly of carbon nanocolloids, Adv. Mater., 19 (2007) 3859–3864.

[29] M. Zhang, Y. Yan, K. Gong, L. Mao, Z. Guo and Y. Chen, Electrostatic layer-by-layer assembled carbon nanotube multilayer film and its electrocatalytic activity for O_2 reduction, Langmuir, 20 (2004) 8781–8785.

[30] M. Zhang, L. Sua and L. Mao, Surfactant functionalization of carbon nanotubes (CNTs) for layer-by-layer assembling of CNT multi-layer films and fabrication of gold nanoparticle/CNT nanohybrid, Carbon, 44 (2006) 276–283.
[31] J. Park, J. Park, S.H. Kim, J. Bang and J. Cho, Desalination membranes from pH-controlled and thermally-crosslinked layer-by-layer assembled multilayers, J. Mater. Chem., (2010) doi: 10.1039/B918921A.
[32] J. Chen, M.A. Hamon, H. Hu, Y. Chen, A.M. Rao, P.C. Eklund and R.C. Haddon, Solution properties of single-walled carbon nanotubes, Science, 282 (1998) 95–98.
[33] S.T. Huxtable, D.G. Cahill, S. Shenogin, L. Xue, R. Ozisik, P. Barone, M. Usrey, M.S. Strano, G. Siddons, M. Shim and P. Keblinski, Interfacial heat flow in carbon nanotube suspensions, Nature Mater., 2 (2003) 731–732.
[34] S. Berber, Y.-K. Kwon and D. Tomanek, Unusually high thermal conductivity of carbon nanotubes, Phys. Rev. Lett., 84 (2000) 4614–4616.
[35] L.X. Benedict, S.G. Louie and M.L. Cohen, Heat capacity of carbon nanotubes, Solid State Commun., 100 (1996) 177–180.